



# Improvement of Plasma Spray Torch Stability by Controlling Pressure and Voltage Dynamic Coupling

V. Rat and J.F. Coudert

(Submitted May 11, 2010; in revised form July 9, 2010)

The development of coating formation processes involving electric arcs depends on process stability and the capacity to ensure a constant reproducibility of coating properties. This is particularly important when considering suspension plasma spraying or solution precursor plasma spraying. Submicron particles closely follow plasma instabilities and have nonhomogeneous plasma treatment. Recently, it has been shown that arc voltage fluctuations in direct-current (dc) plasma torches, showing dominant fluctuation frequencies between 4 and 6 kHz, are linked to pressure oscillations in the cathode cavity of the plasma torch. In this study, first, a method to isolate the different oscillation modes in arc voltage and pressure signals using signal processing methods is presented. Second, correlations between the different modes of oscillations are analyzed following the plasma torch operating parameters. Lastly, it is shown that the use of an acoustic stub, mounted on the torch body, decreases the amplitude of arc voltage fluctuations and slightly increases the mean voltage.

**Keywords** diagnostics and control, influence of spray parameters, nanostructured coatings, nanostructured materials

## 1. Introduction

Conventional direct current (dc) plasma torches are widely used in plasma spraying and have been shown to exhibit strong arc voltage fluctuations (Ref 1-8). The electrical power dissipated within plasma forming gases strongly varies in time, resulting in nonhomogeneous treatment of solid particles injected in the plasma jet (Ref 9). The influence of arc instabilities is very pronounced in cases of suspension plasma spraying or solution precursor plasma spraying because the liquid fragmentation processes depend on local plasma jet properties, especially involved in momentum transfer, changing in time. When studying fragmentation processes at the nozzle exit of a plasma torch using a time-resolved imaging synchronized with the arc voltage, it has been shown that they depend on suspension properties

(e.g., mass load, injection velocity), but also on arc voltage level. Part of the fragmentation products travel in the fringes of the plasma jet, resulting in poorly melted particles in coatings (Ref 10). The treatment of injected or in-flight synthesized submicron particles is also very sensitive to voltage fluctuations because of the low inertia of small solid particles. For example, the characteristic time of momentum change is  $\tau_m = \rho_{\text{part}} d^2 / 18 \mu_p$ , where  $\rho_{\text{part}}$ ,  $d$ , and  $\mu_p$  are, respectively, the particle density, its diameter, and the plasma dynamic viscosity (Ref 11). For a particle immersed within an Ar-H<sub>2</sub> (45-15 vol.%) thermal plasma (10<sup>4</sup> K) with 1  $\mu\text{m}$  diameter,  $\tau_m = 0.8 \mu\text{s}$ . Moreover, the typical period of arc voltage fluctuation for a conventional dc plasma torch is about 200  $\mu\text{s}$ . This means that submicron particles closely follow arc instabilities generated by plasma torches.

For more than four decades, three arc voltage fluctuation modes have been identified for nonconfined arcs, that is, with respect to those generated in plasma spray torches (Ref 1): the steady mode, corresponding to a stable attachment of the arc on the anode wall, the takeover mode, represented by a quasi-sinusoidal time-dependent arc voltage with small amplitudes (a few volts), and the restrike mode. The latter gives a voltage signal approximately saw-tooth in shape. It is the signature of the elongation of electrical current paths due to plasma flow until re-arcing phenomena occur through the cold boundary layer (CBL) between the anode wall and the arc column. During this elongation phase, the electric field in the CBL increases until a new electrical path is initiated by charge-carrier diffusion or electrical breakdown, resulting in a sudden reduction of the arc length connected with an almost instantaneous voltage fall. Then, the sequence arc-elongation/re-arcing is repeated in a more or less regular scheme.

This article is an invited paper selected from presentations at the 2010 International Thermal Spray Conference and has been expanded from the original presentation. It is simultaneously published in *Thermal Spray: Global Solutions for Future Applications, Proceedings of the 2010 International Thermal Spray Conference*, Singapore, May 3-5, 2010, B.R. Marple, A. Agarwal, M.M. Hyland, Y.-C. Lau, C.-J. Li, R.S. Lima, and G. Montavon, Ed., ASM International, Materials Park, OH, 2011.

V. Rat and J.F. Coudert, SPCTS-CNRS UMR 6638, University of Limoges, Limoges, France. Contact e-mail: vincent.rat@unilim.fr.

Later, these studies were extended to confined arcs in plasma torches where similar arc voltage signals were observed in typical operating conditions of plasma spraying. The takeover mode is more easily observed when using monatomic plasma forming gases (argon, helium). The restrike mode is favoured as soon as a molecular gas (hydrogen or nitrogen) is mixed with argon, but it has to be underlined that restrike can also be produced with pure argon by either lowering the arc current or increasing the anode-nozzle diameter. Generally the restrike mode is associated with a point attachment of the arc root at the anode wall, with a transient anchorage during which the surface temperature increases and can reach the melting point, unless the arc attachment moves to another place by re-arcing. The erosion rate is then linked to the characteristic time of heat transfer at the surface under the arc root and the “spot lifetime,” that is the time during which the arc root stays anchored at the same place. This spot lifetime can be identified in the saw-tooth shaped voltage signal as the time that separates two consecutive falls, and it is observed that the individual lifetimes are almost uniformly spread in a range of several tens of  $\mu\text{s}$ . The mean value and the standard deviation that characterize the statistical distribution of spot lifetimes are about the same, which confirms the pronounced random character of re-arcing phenomena. This is caused by the breakdown of the CBL, the thickness of which directly depends on the uncontrolled transverse movements of the arc column and also on the turbulence effects in the arc fringes. However, the mean value of the spot lifetimes, averaged over a few thousands of events, shows a rather well-defined dependence on the operating parameters. Following the aforementioned argument, an increase of the CBL thickness must reduce the probability of re-arcing and the mean value of the spot lifetimes must also increase. In plasma torches, the CBL thickness is the difference between the nozzle channel radius and the arc column radius. The latter increases when the arc current increases and decreases with an increase in the hydrogen content in the plasma gas by enhancing the thermal constriction of the arc column. These facts were confirmed in the past (Ref 2) by specific measurements obtained with a homemade plasma torch and by using different nozzle diameters, arc currents, and gas compositions.

It has to be underlined, at this step, that the mean spot lifetime must not be confused with a hypothetical period of the arc voltage signal, since it results from an average over randomly distributed re-arcing events. This means that the power spectrum of a pure restrike signal gives a noisy spectrum rather than well-resolved spectral lines or peaks.

However, in the case of commercial torches, usually, the arc voltage power spectra display frequency peaks (a few kHz) (Ref 4, 5, 12). Figure 1 shows, for example, the influence of the hydrogen flow rate on arc voltage power spectra for a Sulzer Metco F4 plasma torch. The plasma was generated with an argon (45 slpm)-hydrogen plasma forming gas at 600 A. A main fluctuation frequency is observed between 4 and 5 kHz, and a secondary peak appears at low hydrogen flow rate at about 7.5 kHz. The confusion between the mean arc spot lifetime of the CBL

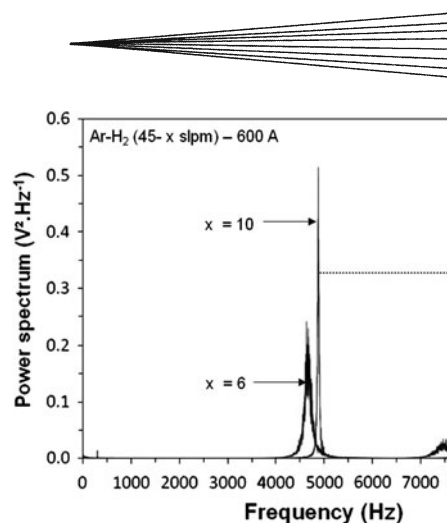


**Fig. 1** Influence of hydrogen flow rate on arc voltage power spectra, Ar-H<sub>2</sub>(45-x slpm), x=5 and 10

approach and the period of the signal obtained from the fluctuation frequency of commercial torches gives rise to a contradiction because the fluctuation frequency increases as the hydrogen flow rate increases. Moreover, according to the voltage signal, the duration of arc restrikes is about 30-100  $\mu\text{s}$ , that is, frequencies higher than 10 kHz. Consequently, the evolution of the main fluctuation frequency (4-5 kHz) cannot be described in terms of CBL thickness.

The examination of arc voltage signal shows that the restrike mode is superimposed on the main fluctuation of arc voltage, that is, that observed around 4-5 kHz. This main oscillation is not only driven by chemico-physical phenomena through the CBL, but is mainly due to compressibility effects of plasma forming gas in the rear part of the plasma torch, that is, in the cathode cavity (Ref 12, 13). The plasma torch behaves like a Helmholtz resonator where pressure, inside the cathode cavity, should be coupled with the arc voltage. In this paper, we present time-resolved pressure measurements inside the cathode cavity, and it is shown that pressure is indeed correlated with the arc voltage. The different modes of oscillation are also extracted by using a numerical Wiener filter. Short-time Fourier transforms allow us to highlight the intermittent behavior of the torch and that the oscillation modes exchange energy. It is also shown that the Helmholtz mode can be damped by the use of an acoustic stub mounted on the plasma torch body. Lastly, the coupling mechanism between voltage and pressure is shown to be linked to the modulation of gas flow rate.

## 2. Experimental Setup

A dc commercial plasma torch (F4 gun, Sulzer Metco) operating at atmospheric pressure, depicted in Fig. 2, was power supplied with a current-regulated source, and the gas feeding rate was controlled by a mass flow meter. The input parameters were the arc current,  $I$ , the gas mass flow rate,  $\dot{m}$ , and the gas composition. The dependent, or output, parameters were the mean arc voltage,  $\bar{V}$ , and the heat

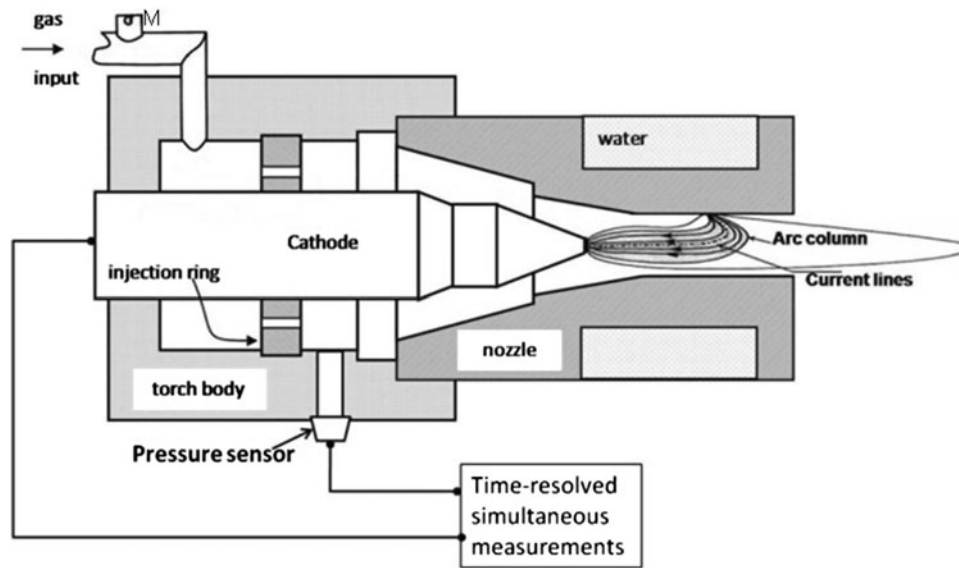


Fig. 2 Direct-current plasma torch

losses to the electrodes,  $\dot{Q}_{\text{loss}}$ . Plasma forming gases were injected through the injection ring in the rear part of the plasma torch. The space between the injection ring and the cathode tip is called “cathode cavity” in this discussion.

Measurements of  $\bar{V}$ ,  $I$ , and  $\dot{Q}_{\text{loss}}$  allowed characterization of the plasma torch (Ref 14), that is, determination of a mean effective specific enthalpy of the plasma jet,  $h_0$ , such as  $h_0 = (\bar{V}I - \dot{Q}_{\text{loss}})/\dot{m}$ . A digital multimeter successively sampled at 50 Hz, with an accuracy of 16 bits, three channels corresponding to the arc voltage, through a dividing bridge, the arc current, using a shunt resistance, and the electrode thermal losses. The latter were deduced from calorimetric measurements performed on the water-cooling system of the plasma torch. A procedure of double averaging on each measurement during approximately 1 min allowed determination of a reliable mean experimental value for each parameter. The multimeter was controlled via a GPIB card by Labview software. The set of values for  $\bar{V}$ ,  $I$ , and  $\dot{Q}_{\text{loss}}$  allowed characterization of each run of the torch in a reproducible way. Then, for each run, time-resolved measurements were performed for the arc voltage,  $U(t)$ , and for the pressure,  $P(t)$ , inside the cathode cavity.

The absolute pressure  $P(t)$  was measured using a piezoresistive sensor (ENDEVCO 8510C, 320 kHz bandwidth, and 4 mm in diameter) inserted in the cathode cavity (see Fig. 2). Arc voltage and pressure of cold gas in the cathode cavity were simultaneously measured with 14 bits of accuracy using a simultaneous data acquisition PCI computer card piloted by Labview software. Because of fast variations of re-arcing phenomena in the plasma torch, signals were sampled at a 320 kS/s rate during 0.2 s, which gave a maximum frequency of 160 kHz and a frequency resolution of 5 Hz.

Section 3 presents results of measurements for arc currents ranging between 400 and 600 A. Argon-hydrogen mixtures were used as plasma forming gases. The hydrogen flow rate varied between 2 and 10 standard liters per

minute (slpm), whereas the argon flow rate was maintained constant at 45 slpm.

### 3. Results

#### 3.1 Helmholtz frequency

A Helmholtz resonator consists of a neck (length  $L$ , cross-section area  $S$ ) connected to a cavity of volume  $V$ . It is based on the oscillating motion of the mass of a gas within the neck due to compressibility effects of gas in the volume  $V$ . The system can be then described in terms of a mass-spring model.

In the approach described here, the cold gas in the cathode cavity is equivalent to the spring, and the plasma in the anode nozzle channel to the oscillating mass (Ref 12), the movements of which are superimposed on the continuous flow.

The Helmholtz frequency,  $f_H$ , is approximated by a simple relationship that includes averaged thermophysical properties of the plasma jet and geometrical data of the plasma torch. It is given by (Ref 12, 13):

$$f_H^2 = \alpha_H \frac{\gamma_g P_g}{\rho_p} \quad (\text{Eq 1})$$

where  $\gamma_g$ ,  $P_g$ , and  $\rho_p$  are, respectively, the isentropic coefficient of the cold gas in the cathode cavity, the mean absolute pressure in the cathode cavity, and the mean plasma density.

The coefficient  $\alpha_H$  is a geometrical parameter given by:

$$\alpha_H = \frac{1}{4\pi^2} \frac{S}{LV_g} \quad (\text{Eq 2})$$

where  $S$ ,  $L$ , and  $V_g$  are, respectively, the area of the cross section of the nozzle channel, the distance between the

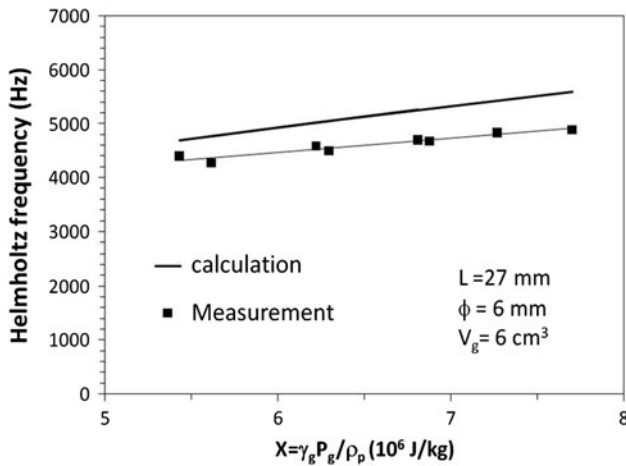


**Fig. 3** Helmholtz frequency measured and calculated from Ref 11 and 12 as a function of  $X = \gamma_g P_g / \rho_p$  defined in Eq 1

cathode tip and the nozzle exit, and the volume of the cathode cavity. In the present study,  $L = 27$  mm and  $V_g = 6$  cm<sup>3</sup>. The internal nozzle diameter is  $\phi = 6$  mm.

The mean absolute pressure is directly measured by the use of the piezoresistive sensor inserted within the cathode cavity. In previous studies, this pressure was approximated by the measurements of mean pressure on the gas feeding line outside the plasma torch (point M) in Fig. 2 and of pressure of cold gas when plasma is not working (Ref 12-14). The measurement of the mean effective specific enthalpy allows us to obtain mean plasma properties using a data bank (Ref 15).

Figure 3 compares the Helmholtz frequency calculated by the use of Eq 1 and 2 including the Rayleigh correction (Ref 12) with that determined from the measured arc voltage power spectra as a function of  $X = \gamma_g P_g / \rho_p$ .

The measured Helmholtz frequency results from an average of power spectra calculated over 20 arc voltage signals. The calculated frequency gives a consistent evaluation of  $f_H$  with the measured one. However, the calculation overestimates  $f_H$  by about 12%.

This discrepancy is due to the geometrical factor calculated from Eq 2 in which the geometrical lengths are not so clearly defined as in the model of Ref 12, 13. In the frame of the model assumptions, the cathode cavity volume and the length of the plasma  $L$  are geometrically well defined.

Figure 4 shows the measured value of  $f_H^2$  and  $\alpha_H$  as a function of  $X$ . A linear evolution is indeed observed where the geometrical parameter is weakly dependent on plasma properties and is 3.24 m<sup>-2</sup>. This latter value gives an experimental signature of the dc plasma torch geometry.

### 3.2 Correlation Between Pressure and Arc Voltage

Figure 5 shows fluctuating components of arc voltage and pressure simultaneously measured for an Ar-H<sub>2</sub> (45-6 slpm) plasma at 600 A. Power spectra of arc voltage highlight different resonances, namely the Helmholtz mode (4-6 kHz), the mode 1 (~7 kHz), and the restrike

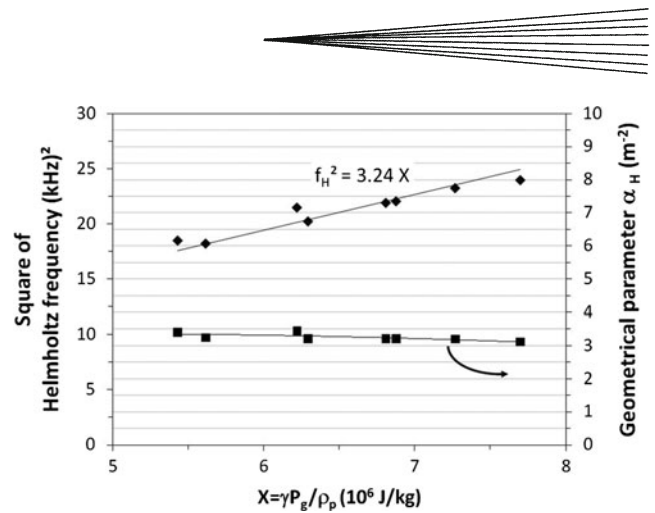


**Fig. 4** Square of Helmholtz frequency and geometrical parameter as a function of  $X = \gamma_g P_g / \rho_p$  defined in Eq 1

mode (Ref 16). In case of pressure, a mode 2 (~16 kHz) was observed.

In order to highlight the coupling between voltage and pressure due to the Helmholtz mode, the latter is extracted from the measured raw signals of arc voltage and pressure using a Wiener filter before finding correlations between voltage and pressure.

It is supposed that the signals of voltage and pressure can be written as

$$s(t) = \sum_i s_i(t)$$

where  $s_i(t)$  are the signals associated with the Helmholtz mode, mode 1 and 2, and restrike mode.

The Wiener filter  $F_i(f)$  of the  $i$ th mode is searched as a real function of frequency and must minimize the Euclidian distance (Ref 17):

$$\frac{\partial}{\partial F_i} \left\{ \int \left\| s_i(t) - TF^{-1}\{F_i(f) \cdot S(f)\} \right\|^2 dt \right\} = 0 \quad (\text{Eq 3})$$

where  $f$  is the frequency,  $t$  is time,  $s_i(t)$  is signal of the  $i$ th mode,  $S(f) = TF\{s(t)\}$  is the Fourier transform of the recorded signal,  $s(t)$ , and  $TF^{-1}$  denotes the reciprocal Fourier transform.

The filter is adapted assuming that power spectral densities of resonance modes (Helmholtz, mode 1, and mode 2) can be approximated by a Lorentzian function to which parameters are fitted using power spectra calculated from signal measurements. Since the restrike mode is randomly distributed in time, it is assumed to be a white noise. Lastly the modes are supposedly noncorrelated because their respective spectral bands do not overlap or their correlation vanishes by phase mixing.

The filter is written with real positive quantities and does not produce phase shifts.

Figure 5 shows the fluctuating component of the raw voltage and pressure signals inside the cathode cavity. In this case, the mean values of voltage and pressure were 54.22 V and  $1.66 \pm 0.02$  bars. With the measurements performed at atmospheric pressure, the amplitude of pressure fluctuations reaching 0.4 bars peak to peak is as

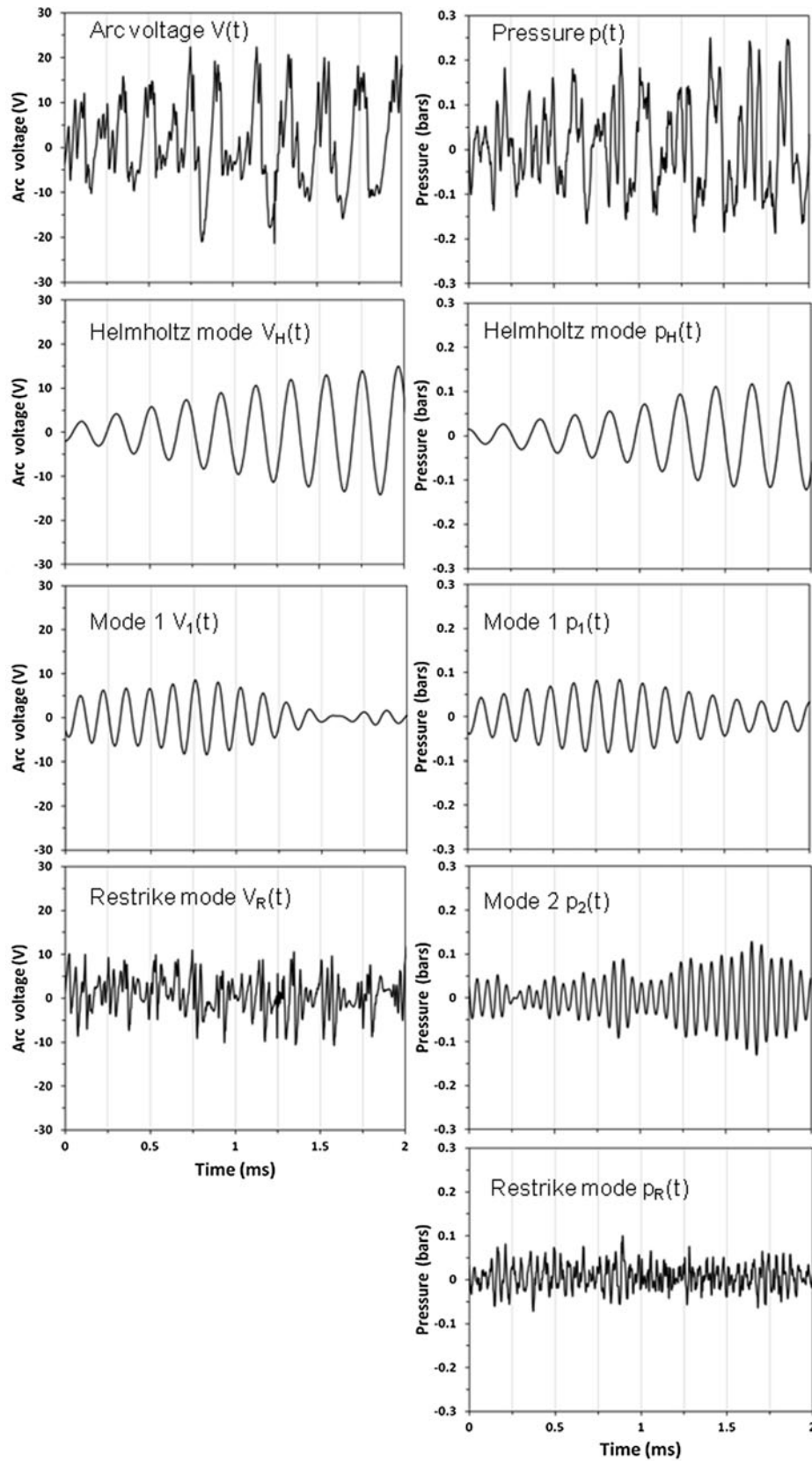


**Fig. 5** Time evolutions of the raw signal (before extraction) and the extracted signals after filtering for arc voltage and pressure in cathode cavity obtained with an Ar-H<sub>2</sub> (45-6 slpm) plasma at 600 A

important as the mean value of the difference of the pressures in the cathode cavity and at the nozzle exit.

The application of the Wiener filter allows extracting the different modes of oscillation, namely Helmholtz mode, mode 1, and restrike mode, which are represented in Fig. 5. The mode 2 is observed only in pressure signals.

The Helmholtz mode in voltage and pressure presents the same evolution and the mode 1 as well. The restrike mode is composed of fast variations of voltage or pressure in less than 50  $\mu\text{s}$ . The signal of the Helmholtz mode presents amplitudes as important as those of the restrike mode, depending on time. The mode 1 is sometimes the dominant mode. Thus, a sort of beating phenomenon is observed transducing a coupling between two oscillators. Short-time Fourier analysis permits highlighting this observation below.

A closer comparison of voltage and pressure of the Helmholtz mode seems to reveal a time shift between both signals. The dependence of this time shift on experimental parameters, namely the arc current and plasma forming gas composition, are discussed in this paper.

This is carried out by calculating the cross-correlation functions between the fluctuating component of the Helmholtz mode of arc voltage,  $v_H(t)$ , and pressure  $p_H(t)$ . The position of the maximum of cross-correlation functions gives the time shift between both signals. This time shift is called propagation time here ( $\tau_p$ ). It is indeed expected that voltage variations cause variation of pressure in the cathode cavity after a propagation time corresponding to the pressure waves traveling from the arc up to the piezoresistive sensor position.

Moreover, the correlation coefficient between the fluctuating component of arc voltage and pressure of the Helmholtz mode, that is,  $v_H(t)$  and  $p_H(t)$ , is calculated as:

$$r = \frac{\sum_i v_H(t_i) p_H(t_i - \tau_p)}{\sqrt{\sum_i v_H^2(t_i)} \sqrt{\sum_i p_H^2(t_i - \tau_p)}} \quad (\text{Eq 4})$$

The correlation coefficient  $r$  is normalized and when  $r$  is equal to 1, the signals are fully correlated; that is, a linear relationship exists between both signals. Nevertheless, a causality relationship does not necessary exist.

Figure 6 presents the dependence of the propagation time  $\tau_p$  and the correlation coefficient  $r$  on the arc current for an Ar-H<sub>2</sub> (45-5 slpm) plasma.

We observe that the propagation time is very weakly dependent on the arc current since it varies between 113 and  $116 \pm 3 \mu\text{s}$  over a wide range of arc current. The correlation coefficient slightly decreases from 0.99 down to 0.98 as the arc current increases. It is very close to unity, indicating a strong correlation between voltage and pressure of the Helmholtz mode.

When increasing the arc current, the plasma properties obviously change. Moreover, it is well known that, in general, the arc radius increases as the arc current increases. However, the propagation time seems to be unchanged. That is why it is assumed that cold gas properties are mainly responsible for the time propagation evolution.

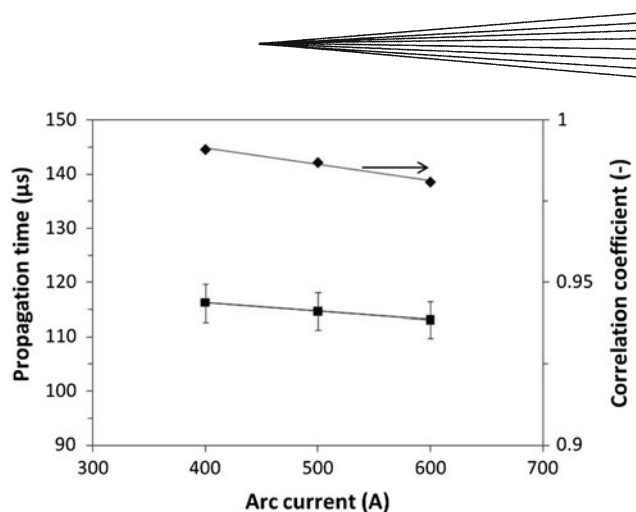


**Fig. 6** Dependence of the propagation time and correlation coefficient between the arc voltage and pressure of the Helmholtz mode on the arc current, Ar-H<sub>2</sub> (45-5 slpm)

We suppose that voltage variations entail pressure changes that propagate from the arc up to the sensor location. However, because of high sound velocity in arc plasma ( $\sim 3000 \text{ m/s}$ ), only the propagation time from the cathode tip up to the sensor location is relevant. That is why the arc current does not really influence the propagation time.

The latter can be written as  $\tau_p = d/(c - w)$ , where  $d$ ,  $c$ , and  $w$  are, respectively, the distance between the cathode tip and the sensor location ( $35 \pm 2 \text{ mm}$ ), the sound velocity in the cold gas, and the cold gas flow velocity in cathode cavity.

The latter,  $w$ , depends on the gas flowing cross-section area and on gas flow rates. However, since the sound velocity ( $\sim 300 \text{ m/s}$ ) is much higher than  $w$  ( $\sim 10 \text{ m/s}$ ),  $w$  is neglected.

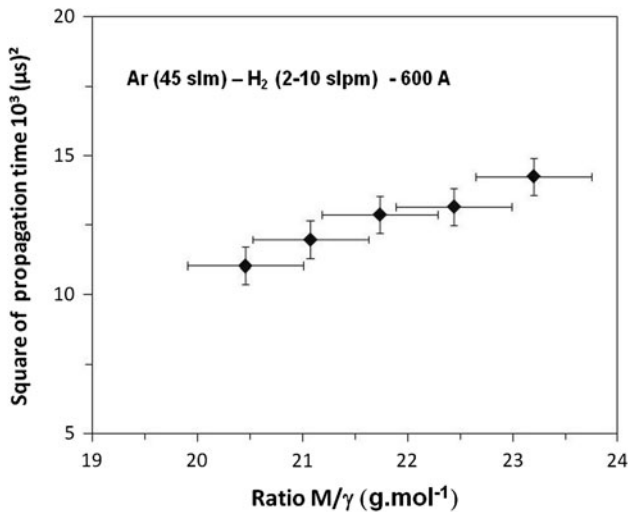
To check the previous assumption, the cold gas properties are modified by changing the hydrogen flow rate from 2 to 10 slpm while keeping constant the argon flow rate (45 slpm). The sound velocity in the cold gas is written:

$$c^2 = \frac{\gamma_g RT}{M} \quad (\text{Eq 5})$$

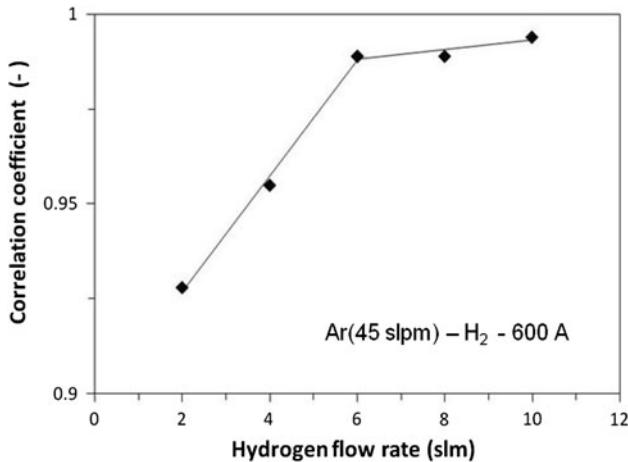
where  $\gamma_g$ ,  $R$ ,  $T$ , and  $M$  are, respectively, the isentropic exponent of plasma forming gases, the ideal gas constant, the temperature of cold gas (300 K), and the molar mass of the mixture.

Figure 7 presents the square of the measured propagation time as a function of  $M/\gamma_g$ . We observe a linear dependence of  $\tau_p^2$ . Moreover, the slope ( $\sim d^2/RT$ ) permits one to deduce the distance between the cathode tip and the sensor location. This distance is found to be 38 mm, which is close to the real distance.

The correlation coefficient is also represented in Fig. 8 for the same operating conditions as Fig. 7 as a function of the hydrogen flow rate. Arc voltage and pressure of the Helmholtz mode are even closely more correlated as the hydrogen content increases because the correlation coefficient changes from 0.93 to 0.99. This means that the Helmholtz resonance is favored as the hydrogen content is increased, which implies more pronounced oscillating



**Fig. 7** Dependence of the square of the propagation time on the ratio of the molar mass and the isentropic coefficient of the cold gas mixture,  $M/\gamma_g$



**Fig. 8** Dependence of the correlation coefficient between the arc voltage and pressure of the Helmholtz mode on hydrogen flow rate

behavior of the arc and larger arc voltage amplitudes. The plasma density decreases as the hydrogen content increases because the specific enthalpy increases, resulting in an increase of the Helmholtz frequency (Eq 1). It is then easier for the plasma to oscillate.

### 3.3 Time-Frequency Analysis of Arc Voltage and Pressure

Time-frequency analysis is a very useful tool to determine how frequency components are distributed in time. The power spectra of arc voltage signal show a frequency component at about 4.5 kHz (Helmholtz mode) and another one at 7.5 kHz (mode 1). Neither the observation of power spectra nor that of raw signals of voltage or pressure permit one to see how both modes are distributed in time.

The short-time Fourier transform (STFT),  $F(t, \omega)$ , consists of calculating power spectra in a sliding window, which explores the whole signal and is defined by:

$$F(t, \omega) = \int_{-\infty}^{+\infty} s(\tau) h(\tau - t) e^{i\omega\tau} d\tau \quad (\text{Eq 6})$$

where  $h$  is a window (Gaussian) and  $s(t)$  can be the arc voltage or pressure.

The spectral resolution depends on the window width and a compromise has to be found between spectral and time resolutions. In this study, the time step is 31  $\mu\text{s}$ , the window width is 7.936 ms, and the signal duration is 0.2 s.

Figure 9 presents short-time Fourier transforms of arc voltage and pressure calculated for an Ar-H<sub>2</sub> (45-6 slpm) plasma generated at  $I=600$  A. It consists of a three-dimensional representation where power spectral densities are displayed as function of time and frequency. Power spectra integrated all over the observation duration are also represented and signals as well.

The arc voltage STFT reveals the intermittent behavior of the plasma torch. If most of the spectral density is distributed in the Helmholtz mode, it can be seen that this mode is interrupted by the mode 1. The plasma torch mainly produces voltage bursts at about 4.5 kHz following the Helmholtz mode, but also at about 7.5 kHz according to the mode 1.

Pressure signal exhibits the same behavior as arc voltage. A good matching for the Helmholtz mode at 4.5 kHz is observed that again proves the correlation between voltage and pressure.

### 3.4 Use of a Tunable "Acoustic Stub" to Modify the Arc Voltage

Indirect proof of the existence of the previously shown coupling between pressure and voltage would be to use an external resonator coupled with the plasma torch itself in order to modify the pressure waves inside the cathode cavity and, consequently, the arc voltage (Ref 18). Figure 10 depicts a tunable "acoustic stub," mounted on the torch body. It is composed of an empty cavity ( $\phi_1 = 10 \pm 0.1$  mm), the depth of which can be varied using the piston position referenced with the  $z$  coordinate. The neck of the acoustic stub ( $\phi_2 = 5 \pm 0.1$  mm,  $h = 6 \pm 0.5$  mm) is connected with the cathode cavity. Plasma forming gases are injected through the injection ring and fill the cavity of the acoustic stub.

The purpose of this study is to highlight the influence of the  $z$  coordinate, that is, the depth of the acoustic stub cavity, on the arc voltage of the plasma torch. Figure 11 displays the time dependence of the arc voltage, generated with an Ar-H<sub>2</sub> (45-10 slpm), 500 A, and a nozzle with a channel inner diameter of 6 mm, on the  $z$  piston position, that is,  $z=0$  and  $1.5 \pm 0.5$  mm. The arc voltages are raw signals and contain all contributions (modes) described previously. The position  $z=0$  mm corresponds to the situation where the acoustic stub is inactive.

In the latter case, typical large amplitudes in arc voltage signal can be observed, which are ascribed to the

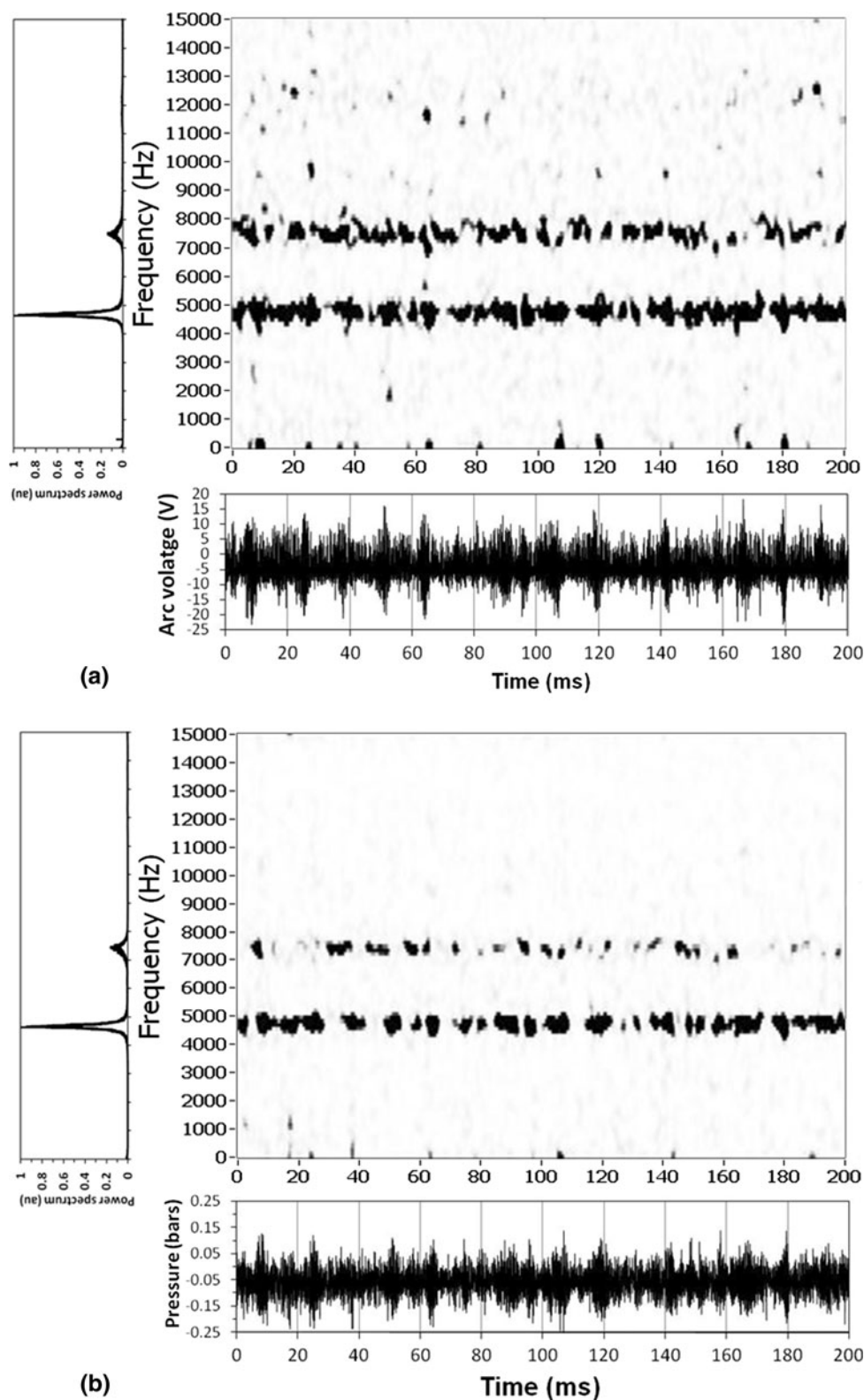


**Fig. 9** Short-time Fourier transforms of (a) arc voltage and (b) pressure. Ar-H<sub>2</sub> (45-6 slpm),  $I=600$  A

Helmholtz mode as explained previously. When  $z = 1.5$  mm, we note that the arc voltage is modified as well as its regular oscillation. The examination of the arc

voltage power spectra shows that the Helmholtz peak, seen for example in Fig. 1, is damped (Ref 18). Consequently, an efficient coupling between the acoustic stub



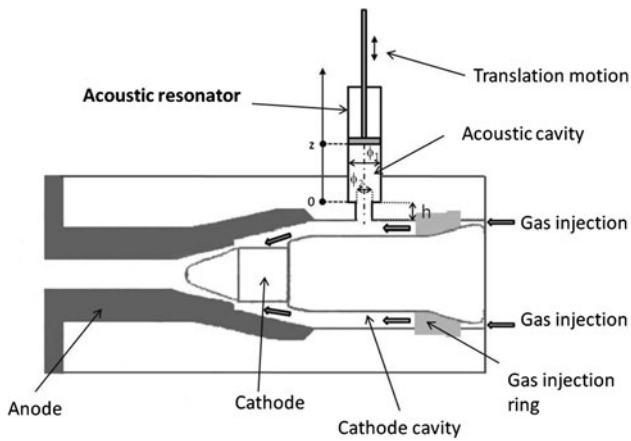


**Fig. 10** Tunable acoustic stub mounted on the torch body

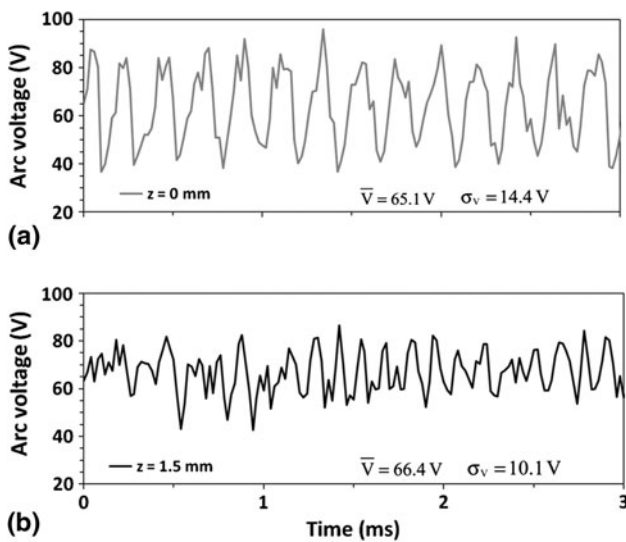


**Fig. 11** Dependence of arc voltage signal [Ar-H<sub>2</sub> (45-10 slpm), 500 A] on  $z$  coordinate giving the piston position of the acoustic stub. (a)  $z = 0$  mm, (b)  $z = 1.5$  mm

and the plasma torch was carried out. The most efficient  $z$  position permitting the Helmholtz mode to be damped was obtained for  $z = 1.5$  mm, but other particular positions were also reported, the difference of which corresponds to the half acoustic wave length of cold plasma forming gases (Ref 18).

Figure 12 shows the dependence of the mean arc voltage on the  $z$  piston positions for the same operating conditions as in Fig. 11. It is shown that the mean arc voltage slightly increases for the previously mentioned particular positions. This confirms the observations of Fig. 11, namely, an increase of voltage minima. It is also interesting to see that, when  $z = 0$  mm, the mean arc voltage is 65 V. This piston position normally corresponds to an inactive acoustic stub. However, we observe that the minimum arc voltage is obtained for 64 V. That is why it is suspected that, even though the acoustic resonator is inactive, the neck ( $h = 6$  mm and  $\phi_2 = 5$  mm) of the latter

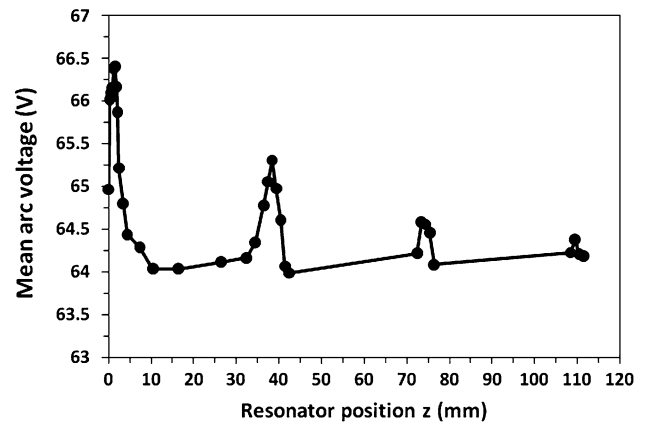


**Fig. 12** Dependence of the mean arc voltage on the  $z$  piston position of the acoustic stub [Ar-H<sub>2</sub> (45-10 slpm), 500 A, internal nozzle diameter 6 mm]

has an active influence on arc voltage. Works are in progress to check this assumption.

### 3.5 Modulation of Gas Flow Rate and Voltage

Previous results have shown the existence of coupling between pressure inside the cathode cavity and arc voltage. However, the question of the coupling mechanism between pressure and voltage is not still elucidated.

It is known that there is a linear dependence, experimentally validated, of mean pressure, measured on the gas feeding line of the plasma torch, on the product  $\dot{m}h_0$  where  $\dot{m}$  and  $h_0$  are, respectively, the gas mass flow rate and the mean specific enthalpy (Ref 14). The latter is obviously linked to the mean arc voltage. A similar dependence between fluctuating components of pressure and voltage signals are expected since the study of cross-correlation functions shows the existence of a time shift between voltage and pressure. It could be ascribed to a propagation time of a mechanical perturbation propagating from the cathode tip up to the piezoresistive sensor position. It means that, when the arc voltage increases, the pressure in the cathode cavity also increases.

Figure 13 shows the pressures measured outside the torch, at point M in Fig. 2 and inside the cathode cavity. The time variations of the latter mean that the amount of gas stored in the cathode cavity fluctuates, because the mass density of the gas fluctuates. It can be seen in Fig. 13, that the ring damps the oscillations so that the pressure in the gas feeding line is almost constant. In addition, the difference between the two aforementioned pressures is responsible for the gas flow rate entering the cathode cavity, through the injection ring. Then, the flow rate entering the arc region must fluctuate because it results from the mass balance of the gas inside cathode cavity, and it can be shown that the gas flow rate in the arc region and the pressure inside the cathode cavity are linked through a first-order differential equation. It is known, from an experimental viewpoint, that an increase of the gas flow rate increases the torch voltage, by an elongation mechanism of the arc column involving friction forces at

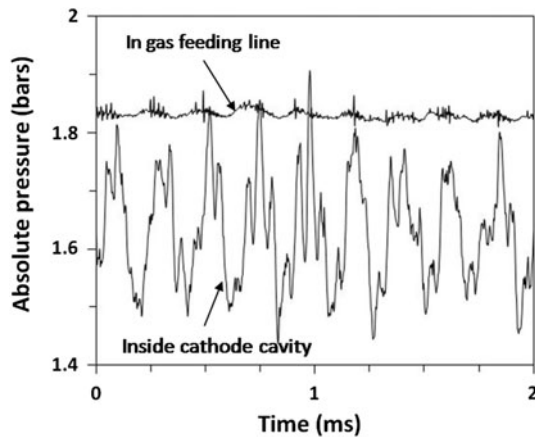


**Fig. 13** Measurements of pressure performed with the same operating conditions (Ar-H<sub>2</sub>, 45-5 slm, 500 A) inside the cathode cavity and in the gas feeding line (point M in Fig. 2)

the arc periphery and also the drag of the arc root at the anode wall. It is then believed that these facts still hold from a dynamic viewpoint, so that the time variations of the pressure are linked to those of voltage, via the fluctuations of the flow rate. This interpretation requires advanced studies taking into account feedback effects, so that the complete behavior of the torch dynamics should obey a closed loop scheme.

## 4. Conclusion

The development of new liquid plasma spraying processes, namely suspension plasma spraying or solution precursor plasma spraying, has renewed the interest to study the electric arc instabilities in dc plasma torches. On the one hand, this is due to liquid fragmentation processes that depend on the time-dependent momentum of the plasma jet. On the other hand, submicron particles or nanosized particles synthesized in flight are very sensitive to plasma fluctuations because of the low thermal and mechanical inertia of these particles.

In this paper, arc instabilities in dc plasma torch were studied. It was shown that they result from the Helmholtz resonance produced by a coupling between the arc itself and pressure in cathode cavity in the rear part of the plasma torch. The main frequency of voltage fluctuations was shown to be dependent on the volume of the cathode cavity (Ref 12, 13). Pressure inside the cathode cavity was simultaneously measured with the arc voltage to establish correlations between both signals. Time signals exhibit several contributions, the Helmholtz mode, modes 1 and 2, and the restrike mode. Modes 1 and 2 have unclear origins that could be ascribed to acoustic resonances in the plasma torch. A numerical Wiener filter applied to measured signals allowed extracting the Helmholtz mode that is the most important contribution in signals. The calculation of cross-correlation functions between voltage and pressure of the Helmholtz mode has shown that both

signals are time shifted, which seems to correspond to a propagation time of pressure waves traveling from the cathode tip up to the sensor location. The correlation coefficients between voltage and pressure signals show a strong correlation between them.

Short-time Fourier transforms have highlighted the strongly transient behavior of the plasma torch which, in reality, works following several resonance modes that exchange energy. A typical beating phenomenon is observed, indicating that at least two oscillators are coupled in the plasma torch, probably the Helmholtz mode and mode 1. This last statement is backed by recent works consisting in using an acoustic stub to modify the arc voltage (Ref 18). This acoustic stub is mounted on the torch body and connected to the cathode cavity. It permits one to significantly reduce the mean relative amplitude of arc voltage. Meanwhile, the previous beating phenomenon in the envelope of the arc voltage signal is altered by the use of the acoustic stub, showing it is indeed coupled with the plasma torch.

Lastly it is suggested that the coupling mechanism between arc voltage and pressure could be, at least partly, due to a modulation of gas flow rate imposed by the pressure fluctuations.

## References

1. S.A. Wutzke, E. Pfender, and E.R.G. Eckert, Study of Electric-Arc Behaviour with Superimposed Flow, *AIAA J.*, 1967, **5**(4), p 707-713
2. J.F. Coudert, M.P. Planche, and P. Fauchais, Characterization of D.C. Plasma Torch Voltage Fluctuations, *Plasma Chem. Plasma Process.*, 1996, **16**(1), p 211S-227S
3. M. Hrabovsky, M. Konrad, V. Kopecky, J. Hlina, J. Benes, and E. Vesely, Motion of Anode Attachment and Fluctuations of Plasma Jet in DC Arc Plasma Torch, *High Temp. Mater. Process.*, 1997, **1**, p 167-178
4. J.L. Dorier, M. Gindrat, C. Hollenstein, A. Salito, M. Loch, and G. Barbezat, Time-Resolved Imaging of Anodic Arc Root Behavior During Fluctuations of DC Plasma Spraying Torch, *IEEE Trans. Plasma Sci.*, 2001, **29**(3), p 494-501
5. Z. Duan and J. Heberlein, Arc Instabilities in a Plasma Spray Torch, *J. Therm. Spray Technol.*, 2002, **11**(1), p 44-51
6. S. Ghorui and A.K. Das, Origin of Fluctuations in Atmospheric Pressure Arc Plasma Devices, *Phys. Rev. E*, 2004, **69**, p 026408
7. G. Mauer, J.L. Marqués-López, R. Vaßen, and D. Stöver, Detection of Wear in One-Cathode Plasma Torch Electrodes and Its Impact on Velocity and Temperature of Injected Particles, *J. Therm. Spray Technol.*, 2007, **16**(5-6), p 933-939
8. J.P. Trelles, E. Pfender, and J.R.V. Heberlein, Modelling of the Arc Attachment Process in Plasma Torches, *J. Phys. D Appl. Phys.*, 2007, **40**, p 5635-5648
9. J.F. Bisson, B. Gauthier, and C. Moreau, Effect of Plasma Fluctuations on In-Flight Particle Parameters, *J. Therm. Spray Technol.*, 2003, **12**(1), p 38-43
10. R. Etchart-Salas, V. Rat, J.F. Coudert, P. Fauchais, N. Caron, K. Wittman, and S. Alexandre, Influence of Plasma Instabilities in Ceramic Suspension Plasma Spraying, *J. Therm. Spray Technol.*, 2007, **16**(5-6), p 857-865
11. C. Crowe, M. Sommerfeld, and Y. Tsuji, *Multiphase Flows with Droplets and Particles*, CRC Press, Boca Raton, 1998
12. J.F. Coudert, V. Rat, and D. Rigot, Influence of Helmholtz Oscillations on Arc Voltage Fluctuations in a dc Plasma Spraying Torch, *J. Phys. D Appl. Phys.*, 2007, **40**, p 7357-7366

13. J.F. Coudert and V. Rat, Influence of Configuration and Operating Conditions on the Electric Arc Instabilities of a Plasma Spray Torch: Role of Acoustic Resonance, *J. Phys. D Appl. Phys.*, 2008, **41**, p 205-208
14. V. Rat and J.F. Coudert, A Simplified Analytical Model for dc Plasma Spray Torch: Influence of Gas Properties and Experimental Conditions, *J. Phys. D Appl. Phys.*, 2006, **39**, p 4799-4807
15. B. Pateyron, TTWinner Free Download from <http://www.unilim.fr/spcts> or <http://ttwinner.free.fr>
16. V. Rat and J.F. Coudert, Pressure and Arc Voltage Coupling in dc Plasma Torches: Identification and Extraction of Oscillation Modes, *J. Appl. Phys.*, 2010, **108**(3), p 043304
17. J.F. Coudert, M.P. Planche, and P. Fauchais, Velocity Measurement of dc Plasma Jets Based on Arc Root Fluctuations, *Plasma Chem. Plasma Process.*, 1995, **15**(1), p 47-70
18. V. Rat and J.F. Coudert, Acoustic Stabilization of Electric Arc Instabilities in Non-transferred Plasma Torches, *Appl. Phys. Lett.*, 2010, **96**, p 101503